Hindawi Publishing Corporation
International Journal of Photoenergy
Volume 2014, Article ID 380120, 8 pages
http://dx.doi.org/10.1155/2014/380120

Research Article

Improved Performance for Dye-Sensitized Solar Cells Using a Compact TiO_2 Layer Grown by Sputtering

Hung-Chih Chang,[1] Ming-Jenq Twu,[2] Chun-Yao Hsu,[3] Ray-Quen Hsu,[1] and Chin-Guo Kuo[4]

[1] *Department of Mechanical Engineering, National Chiao Tung University, 1001 Ta Hsueh Road, Hsinchu 30010, Taiwan*
[2] *Department of Mechatronic Engineering, National Taiwan Normal University, 162 Heping East Road, Section 1, Taipei 10610, Taiwan*
[3] *Department of Mechanical Engineering, Lunghwa University of Science and Technology, No. 300, Section 1, Wanshou Road, Guishan, Taoyuan 33306, Taiwan*
[4] *Department of Industrial Education, National Taiwan Normal University, 162 Heping East Road, Section 1, Taipei 10610, Taiwan*

Correspondence should be addressed to Chin-Guo Kuo; chinguo7@yahoo.com.tw

Received 22 March 2014; Accepted 5 April 2014; Published 22 May 2014

Academic Editor: Ho Chang

This work determines the effect of compact TiO_2 layers that are deposited onto fluorine-doped tin oxide (FTO), to improve the performance of dye-sensitized solar cells (DSSC). A series of compact TiO_2 layers are prepared using radio frequency (rf) reactive magnetron sputtering. The films are characterized using X-ray diffraction (XRD), atomic force microscopy (AFM), scanning electron microscopy (SEM), and UV-Vis spectroscopy. The results show that when the $Ar/O_2/N_2$ flow rates are 36 : 18 : 9, the photo-induced decomposition of methylene blue and photo-induced hydrophilicity are enhanced. After annealing at 450°C in an atmosphere ambient for 30 min, the compact TiO_2 layers exhibit higher optical transmittance. The XRD patterns for the TiO_2 films for FTO/glass show a good crystalline structure and anatase (101) diffraction peaks, which demonstrate a higher crystallinity than the ITO/glass films. As a result of this increase in the short circuit photocurrent density, the open-circuit photovoltage, and the fill factor, the DSSC with the FTO/glass and Pt counter electrode demonstrates a solar conversion efficiency of 7.65%.

1. Introduction

Photocatalytic TiO_2 materials are widely used in antipollution applications, deodorization, dust-proofing, and for high-performance dye-sensitized solar cells (DSSC) because of their unique physical, chemical, and optical properties, their lack of toxicity, and low cost [1]. The energy gap for titanium dioxide for photocatalysts is about 3.2 eV, so ultraviolet excitation causes electrons to jump to the conduction band to form electron-hole pairs. The holes formed in the catalyst are used to degrade organic materials or undesired pollutants for antipollution, deodorization, and antibacterial uses [2, 3]. Because N-doped TiO_2 (TiO_2:N) powders or thin films have better photocatalytic properties than undoped TiO_2 films [4], some studies have added nitrogen gas during the growth of TiO_2 films, to increase the photocatalytic activity of TiO_2 in the visible-light region [5, 6]. Using N-doped TiO_2 results in significant improvements in the visible light response and photocatalytic degradation [7].

Since the first report of a DSSC by O'Regan and Grätzel, in 1991 [8], they have been intensively studied as a potential replacement for standard solar cells because of their relatively high efficiency and low cost [9], compared with p-n junction photovoltaic devices [10, 11]. A typical DSSC consists of dye molecules that act as sensitizers, a porous TiO_2 layer, a fluorine-doped tin oxide (FTO) substrate, an electrolyte charge carrier, and a platinized FTO substrate as a so-called counter electrode or cathode. The structure, morphology and crystalline phases of TiO_2 play an important role in the performance of DSSC's. The nano-sized porous structure TiO_2 layer is widely used as an electrode in DSSC, to allow a high density of dye molecules to be embedded onto the TiO_2 surface and enhance the photo absorption process [12]. However, the porous structure of the TiO_2 layer

Table 1: The deposition conditions for TiO_2.

Substrate	nonalkali glass $25 \times 25 \times 1\,mm^3$			
Target	Ti (99.99% purity)			
Gas	Ar, O_2, N_2 (99.99% purity)			
Base pressure	5.0×10^{-6} torr			
Spin speed of the substrate	10 rpm			
Substrate-to-target distance	80 mm			
rf power	100 W			
Sputtering pressure	10 mtorr			
Substrate temperature	300°C			
Sample	Ar flow rate (mL/min)	O_2 flow rate (mL/min)	N_2 flow rate (mL/min)	$Ar : O_2 : N_2$
Number 1	35	35	0	1 : 1 : 0
Number 2	48	24	0	2 : 1 : 0
Number 3	54	18	0	3 : 1 : 0
Number 4	20	20	20	1 : 1 : 1
Number 5	29	29	14	1 : 1 : 0.5
Number 6	25	25	8	1 : 1 : 0.33
Number 7	27	14	14	2 : 1 : 1
Number 8	36	18	9	2 : 1 : 0.5
Number 9	36	18	6	2 : 1 : 0.33
Number 10	45	14	14	3 : 1 : 1
Number 11	45	15	7	3 : 1 : 0.5
Number 12	41	14	4	3 : 1 : 0.33

can cause an electrical short between the liquid electrolyte and the FTO substrate, which leads to a decrease in cell efficiency. A potential means of preventing recombination is the application of a compact metal-oxide film between the nano-sized porous TiO_2 layer and the FTO substrate. Of these metal oxides, TiO_2 is the most effective electrolyte blocker and has been extensively studied [13, 14]. This compact layer improves the adhesion of the porous TiO_2 to the FTO substrate and provides a larger TiO_2/FTO contact area and more effective electron transfer from the porous TiO_2 to the FTO by preventing the electron recombination process [15]. A compact TiO_2 layer is prepared using many growth techniques, such as sputtering, chemical vapor deposition, spin-coating, or spray pyrolysis. In particular, the compact TiO_2 layer produced by sputtering deposition is simple and inexpensive and is widely used in DSSC studies [16, 17].

This study determines the carrier blocking effect of a compact TiO_2 layer that is deposited onto a FTO substrate, using radio frequency (rf) reactive magnetron sputtering, with a Ti metal target, Ar as the plasma gas and O_2 and N_2 as the reactive gases. The effect of the $Ar/O_2/N_2$ flow ratios on the structure, surface morphology, photocatalytic activity, and DSSC conversion efficiency of TiO_2 thin films is studied. The nano-sized porous TiO_2 layer is coated using the sol-gel process and calcination at 450°C and 500°C. The working electrode is a dye-sensitized TiO_2 film that is immobilized on a fluorine-doped tin oxide (FTO) substrate. The Pt and carbon counter electrode are coated onto FTO/glass substrates.

2. Experiments

Compact TiO_2 layers were coated onto FTO/glass substrates (nonalkali glass, $25 \times 25 \times 1\,mm^3$) by rf reactive magnetron sputtering from a high purity Ti target in an $Ar/O_2/N_2$ atmosphere, using a constant sputtering pressure (10 mtorr), rf power (100 W), substrate temperature (300°C) and distance between the substrate and the target (80 mm), and variable flow rates for argon, oxygen, and nitrogen. All of the samples were deposited by rotating the substrate (10 rpm), to ensure good surface morphology. Before deposition, the system was evacuated to a pressure of less than 5.0×10^{-6} torr. The detailed deposition conditions are listed in Table 1. The substrates were cleaned, in acetone, using ultrasound, rinsed with deionized water, and dried in nitrogen. Samples 1–3 (TiO_2) were deposited in an Ar/O_2 atmosphere, without nitrogen gas. Samples 4–12 ($TiO_{2-x}N_x$) were deposited in an $Ar/O_2/N_2$ atmosphere and nitrogen gas was added in different fractions. The TiO_2 films were characterized by their deposition rates, hydrophilic properties, photocatalytic behavior, and morphology.

The porous TiO_2 film was coated onto the compact TiO_2/FTO/glass using a mixture of P-25 with the TiO_2 sol-gel component studied in [18, 19]. The TiO_2 sol-gel was mixed with 0.3 g of commercially available Degussa P-25, to avoid any cracking of the film. The gels were predried for 20 min at 50°C and then sintered in a furnace at 450°C and 500°C (heating rate 10°C/min) for 30 min in air ambient, to produce the bare TiO_2 electrode used in this work to fabricate the

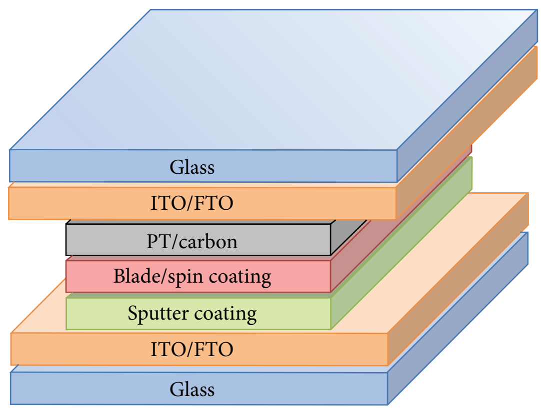

Figure 1: The structure of an assembled DSSC with a sputtered compact TiO_2 layer/FTO/glass and other layers.

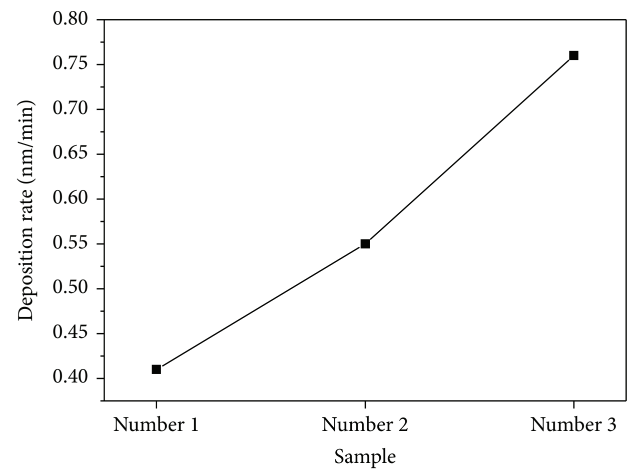

Figure 2: The TiO_2 deposition rate for samples number 1, number 2, and number 3 (without nitrogen addition).

DSSC. The porous TiO_2 films were immersed into the dye (N 719) complex, for 24 h at room temperature [20, 21].

The Pt and carbon counter electrode was coated onto FTO/glass substrates using DC sputtering with pure Ar gas and a DC power of 30 W. The dye-adsorbed TiO_2 working electrode and the counter electrode were assembled into a sandwich-type cell and sealed with a hot-melt sealant. Figure 1 shows a schematic diagram of a DSSC with a sputtered compact TiO_2 layer/FTO/glass. Dense TiO_2 passivating layers were used to prevent any leakage to the liquid electrolyte by electron transfer.

The photo-induced hydrophilicity was evaluated using contact angle measurements to pure water, which were performed at room temperature in an ambient atmosphere, using a contact angle meter (FACE CA-VP150) with an experimental error of less than 1°. The photocatalytic behavior of the TiO_2 coatings was assessed using a combination of ultraviolet irradiation and absorption measurements. The TiO_2 was placed in 10 μM methylene blue (MB) aqueous solution and irradiated for 4 hours, using 1.5 mW/cm^2 UV lights. The observed photodecomposition of the aqueous solution is seen in the UV-Vis spectrum (measured using a UVP UVL-225D with a wavelength range of 300–800 nm) as a decrease in the maximum absorbance as the irradiation increases. The film thickness and crystal structure were, respectively, measured using α-step (surface profiler system, Dektat) and XRD (Rigaku-2000). The morphology and the roughness were determined using SEM (JEOL JSM-6500F) and AFM (SPA 400).

The power used to test the prepared DSSC was a 150 W Xe lamp, which simulates sunlight (AM 1.5). Before the test, the distance between the light source and the sample was adjusted to allow a light source density of 100 mW/cm^2. The cell performance parameters, including the short-circuit current density (J_{sc}), the open-circuit voltage (V_{oc}), the fill factor (FF), and the photoelectronic conversion efficiency (η (%) = $J_{sc} \times V_{oc} \times$ FF/total incident energy × 100), were measured and calculated using the J-V characteristics of DSSC's.

Table 2: The deposition rate and roughness value for the TiO_2 films.

Samples	Deposition rate (nm/min)	Roughness, Ra (nm)
Number 1	0.41	0.32
Number 2	0.55	0.33
Number 3	0.76	0.44
Number 4	0.86	0.35
Number 5	0.65	0.47
Number 6	0.73	0.77
Number 7	0.79	2.77
Number 8	0.89	1.21
Number 9	0.75	2.25
Number 10	0.68	4.12
Number 11	0.71	3.95
Number 12	0.82	2.89

3. Results and Discussion

3.1. Characteristics of TiO_2 Obtained by rf Reactive Sputtering. The TiO_2 photocatalytic thin films deposited on glass substrates demonstrate very good adherence. No cracking or peel off is observed after deposition. Figure 2 shows the deposition rates for samples number 1, number 2, number and 3. These three samples (where nitrogen was added) were deposited using O_2 flow-rate ratios from 35 to 18 mL/min (see Table 1). The deposition rate increases as the O_2 partial pressure decreases. Greater oxygen flow increases the probability of collision with Ar^+ ions and decreases the energy of the Ar^+ ions that bombard the Ti surface. Increasing the O_2 flow rate also results in a significant decrease in the sputtering voltage [22]. Therefore, the dissociation gas is reduced, along with the plasma density and the deposition rate. Table 2 shows the deposition rates and roughness values for all samples. For nitrogen-doped samples, the roughness is increased when the Ar flow fraction is increased.

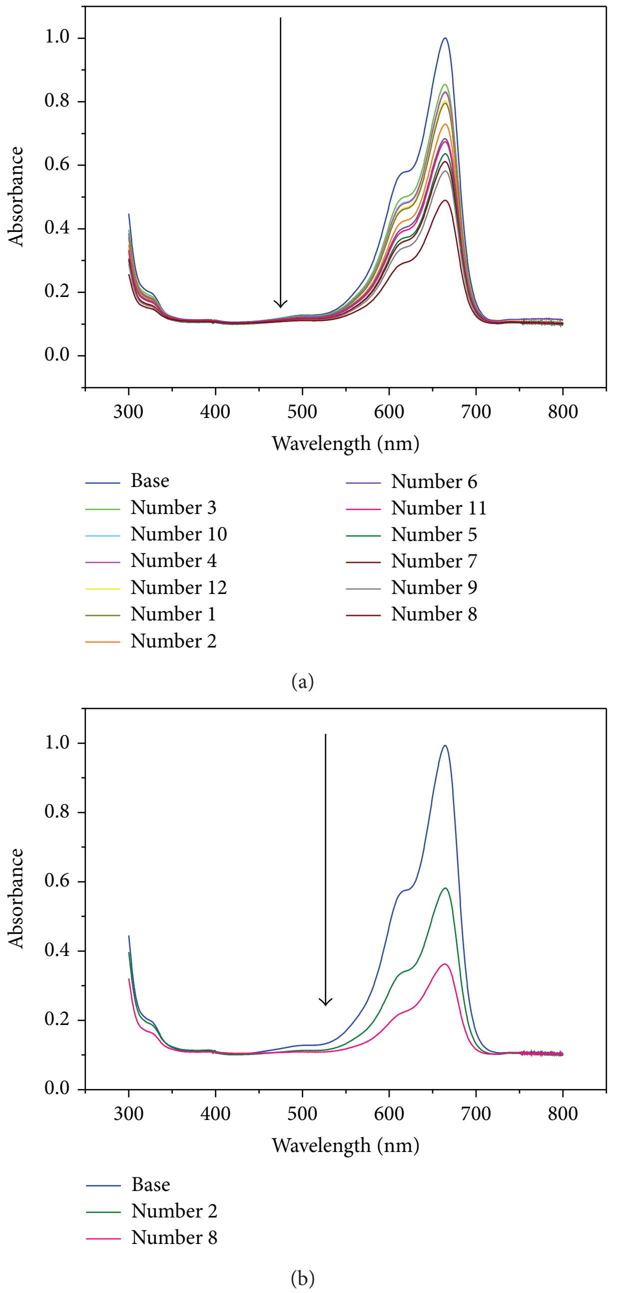

Figure 3: The absorption spectrum for MB aqueous solution ($10\,\mu$M, pH = 7.0), after UV irradiation for 4 h: (a) samples 1–12 and (b) samples number 2 and number 8.

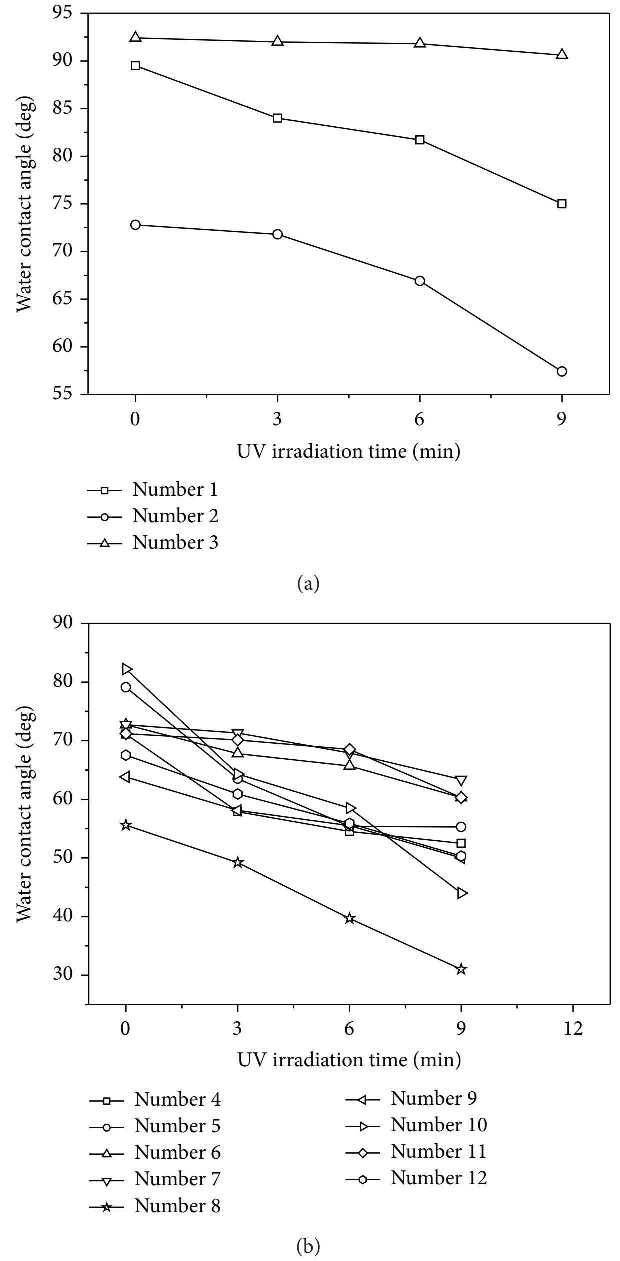

Figure 4: The change in the water contact angle after UV irradiation: (a) without nitrogen addition and (b) with nitrogen addition.

Figure 3(a) shows the absorption spectrum for MB under UV irradiation for 4 h, for films deposited under various coating conditions. If no nitrogen is added during the deposition process, the best degradation of MB is demonstrated by sample number 2, with a MB absorbance of 0.74. When nitrogen is added during the deposition process, the best absorbance of MB is 0.54, for sample number 8. The deposition parameters for sample number 8 are a rf power of 100 W, a deposition pressure of 10 mtorr, an $Ar/O_2/N_2$ flow rate of 36/18/9 mL/min, and substrate temperature of 300°C. Figure 3(b) shows the absorption spectrum of MB under visible light irradiation for 4 h for the deposited film samples number 2 and number 8. This result shows that $TiO_{2-x}N_x$ exhibits photocatalytic characteristics and the MB degradation of $TiO_{2-x}N_x$ film is better than that of TiO_2 film.

Figures 4(a) and 4(b) show the change in the water contact angle after UV irradiation for 9 min, without and with the addition of nitrogen, respectively. Figure 4(a) shows that the contact angles for the TiO_2 films decrease by 1°, 14°, and 13°, for samples number 1, number 2 and, number 3, respectively, after UV irradiation for 9 min. Figure 4(b) shows that the average contact angle for $TiO_{2-x}N_x$ film deposited

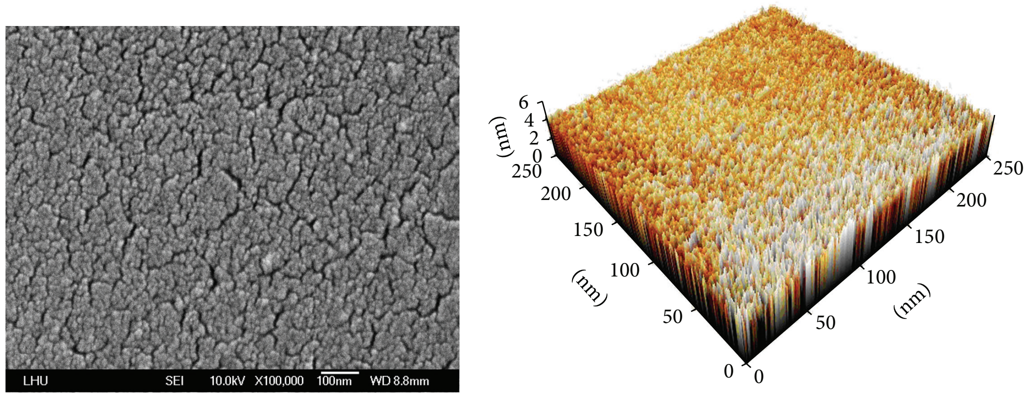

Figure 5: The SEM and AFM images for sample number 2.

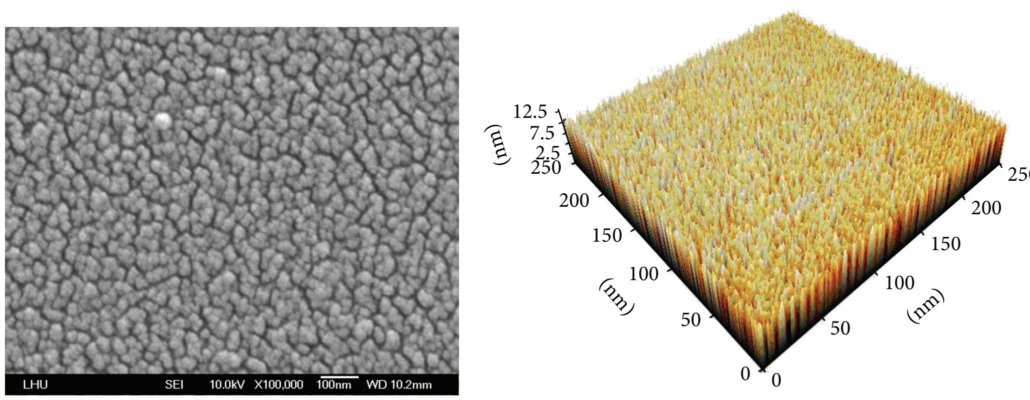

Figure 6: The SEM and AFM images for sample number 8.

with the addition of nitrogen is 20° less after UV irradiation. This result shows that the photo-induced hydrophilicity of $TiO_{2-x}N_x$ film is better than that of TiO_2 film.

The best degradation occurs for samples number 2 and number 8, without and with nitrogen addition, respectively, as determined by AFM and SEM. Figures 5 and 6 show the morphology of samples number 2 and number 8, respectively. The columnar structures of the two films are identified using AFM. The respective roughness (R_a) values for samples number 2 and number 8 are 0.33 nm and 1.21 nm (see Table 2). The atomic number ratio for the surface and the volume is an important parameter for photocatalytic properties. A higher ratio results in greater photocatalytic activity. When the roughness value decreases, the photocatalytic activity decreases, because there is less surface area. In contrast, when the roughness is greater, the photocatalytic activity is greater, because there is a larger surface area.

3.2. DSSC Characterization. Figure 7 shows the transmittance spectra as a function of wavelengths in the visible range for compact TiO_2 layers. After annealing at 450°C in an atmosphere ambient for 30 min, the compact TiO_2 layers demonstrate higher optical transmittance. However, when the annealing temperature is 500°C, the optical transmittance decreases slightly.

SEM analysis was used to determine the morphology of the TiO_2 porous layer produced using the sol-gel method onto the compact TiO_2 layers (sputtered with $Ar/O_2/N_2$ flow rates of 36 : 18 : 9: sample number 8)/FTO substrate, as shown in Figure 8. The samples were annealed at 450°C in an atmosphere ambient for 30 min. After sputtering the compact TiO_2 layers are dense and evenly coated to prevent charge recombination, which adheres to the electrode surface strongly (Figure 8(a)). The SEM images show the porous TiO_2 film over the sputtered compact layer that is produced using sol-gel with spin coating has proper density and the crystallite size (Figure 8(b)), which gives a more efficient DSSC. The cross-section of the films was observed by SEM. Figure 9(a) corresponds to Figure 8(b) and Figure 9(b) corresponds to Figure 8(c). These results confirm a sponge-like structure for the TiO_2 layer, which is a prerequisite for a highly efficient DSSC. Figure 10 shows the XRD patterns

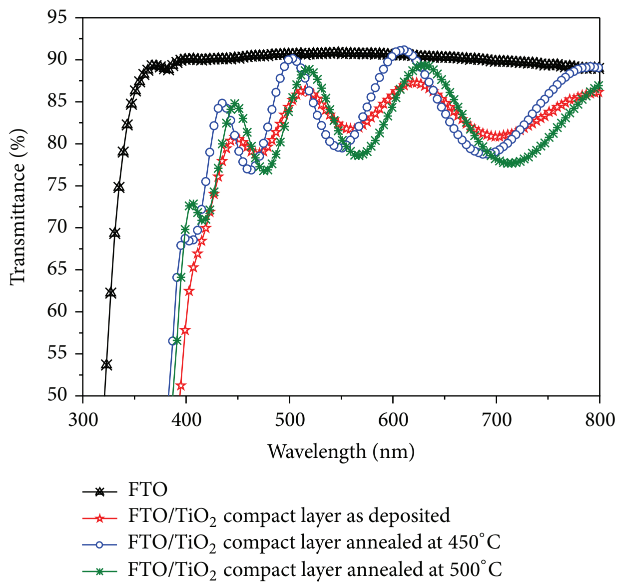

Figure 7: The optical transmittance spectra for a compact TiO_2 layer/FTO/glass.

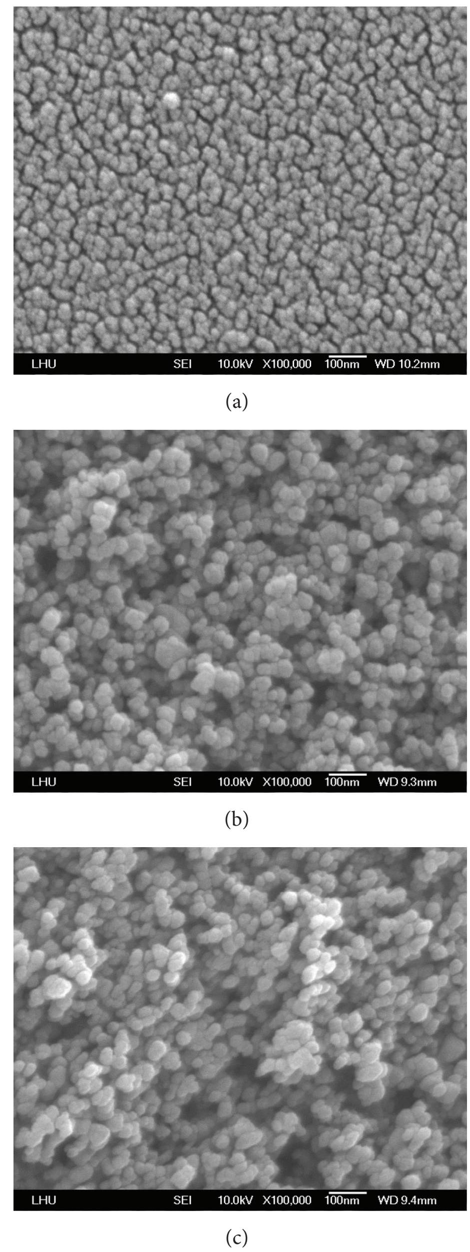

Figure 8: The SEM images of (a) sputtered TiO_2 compact layer on FTO/glass (sample number 8), (b) porous TiO_2 on TiO_2 compact layers/FTO/glass, produced using the sol-gel with spin coating method and (c) porous TiO_2 on compact TiO_2 layers/FTO/glass, produced using the sol-gel with blade coating method.

for the TiO_2 films. FTO/glass shows a good crystalline structure and anatase (101) diffraction peaks that have a higher crystallinity than the ITO/glass films.

In order to compare the performance of a DSSC fabricated on the FTO/glass substrate and the ITO/glass substrate, using Pt counter electrodes and carbon counter electrodes [23], a conventional DSSC was prepared, as shown in Figure 11. Figure 11 shows the photocurrent-voltage (J-V) characterization of the DSSC with a sputtered compact TiO_2 layer, under AM 1.5 solar irradiation with a density of 100 mW/cm^2. The performance parameters are summarized in Table 3. The short circuit photocurrent density (J_{sc}), the open-circuit photovoltage (V_{oc}), and the fill factor for the FTO/glass substrate using Pt counter electrodes are greater than those for the other samples. With ITO/glass, using the carbon counter electrodes, conversion efficiency decreases to 1.51%, from 4.98%, for Pt counter electrodes. This increase in the J_{sc}, the V_{oc}, and the fill factor means that the DSSC with the FTO/glass and a Pt counter electrode has a solar conversion efficiency of 7.65%, compared with 4.98% for the cell prepared using ITO/glass.

4. Conclusions

This study successfully deposits TiO_2 and $TiO_{2-x}N_x$ onto ITO/glass and FTO/glass substrates. The flow rates for Ar (plasma gas), O_2, and N_2 (reactive gases) are varied, but the rf power, the deposition pressure, and the substrate temperature are fixed. The results show that the photo-induced hydrophilicity of $TiO_{2-x}N_x$ film is better than that of TiO_2 film. The best absorbance of methylene blue (MB) is 0.54, for sample number 8 (the $Ar/O_2/N_2$ flow rates are 36 : 18 : 9), after UV irradiation for 4 h. This result shows that MB degradation for $TiO_{2-x}N_x$ film is better than that for TiO_2 film. After annealing, the compact TiO_2 layers exhibit higher optical transmittance. The TiO_2 porous layer on the TiO_2 compact layers/FTO substrate produced using the sol-gel method exhibits a sponge-like structure, which is a prerequisite for a highly efficient DSSC. For ITO/glass with carbon counter electrodes, the conversion efficiency decreases to 1.51%, from 4.98% for Pt counter electrodes. The short circuit photocurrent density (J_{sc}), the open-circuit

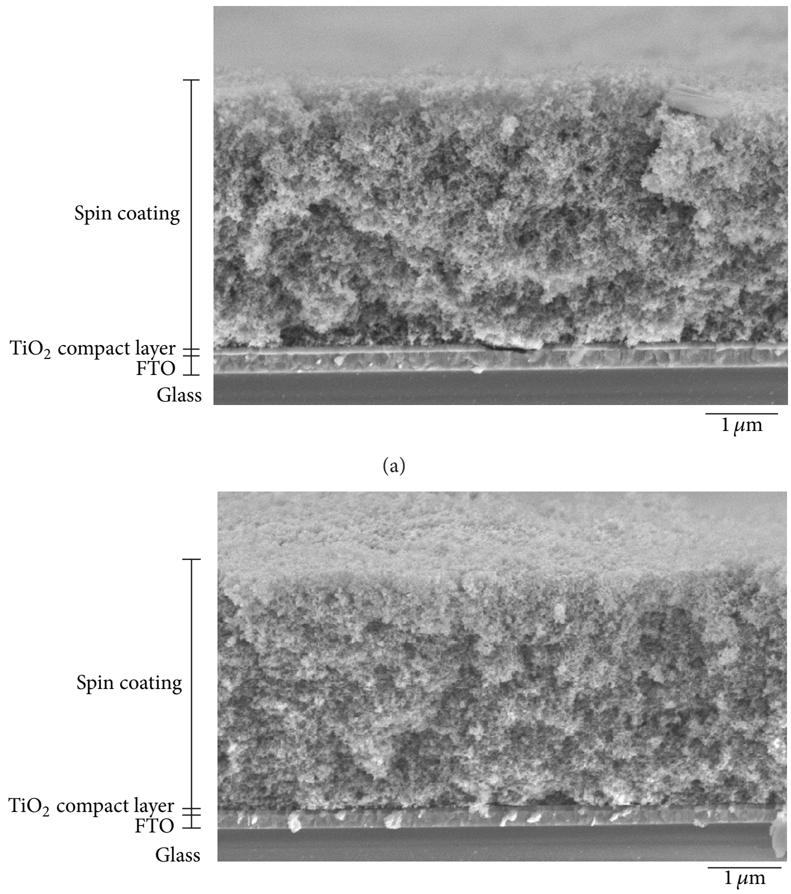

FIGURE 9: The SEM cross-sectional image (a) corresponding to Figure 8(b) and (b) corresponding to Figure 8(c).

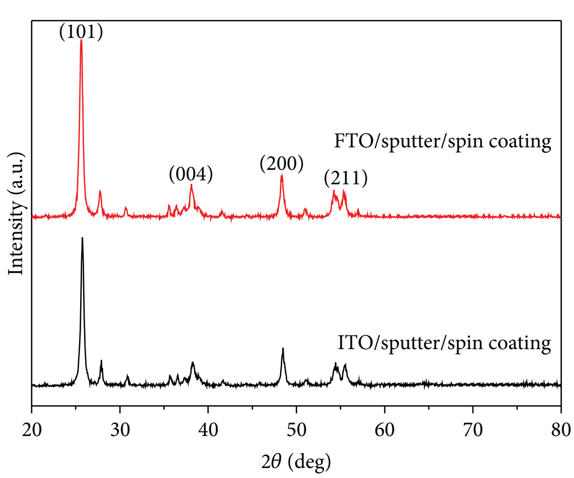

FIGURE 10: The XRD patterns for the TiO_2 films, annealed at 450°C.

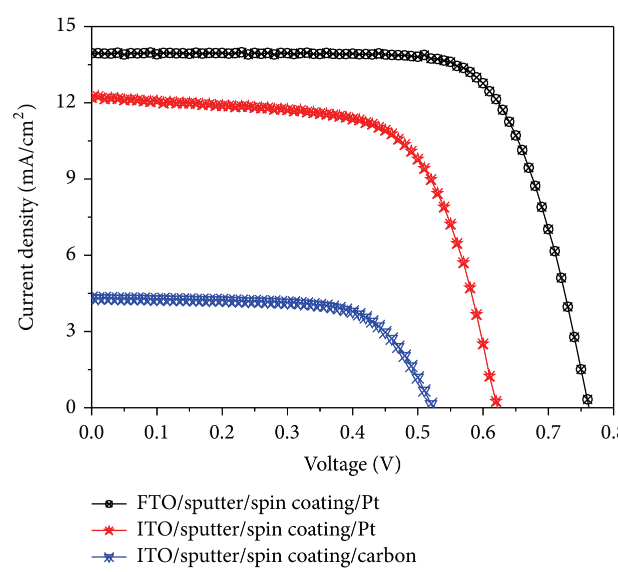

FIGURE 11: Current-voltage plots for the DSSC with a sputtered compact TiO_2 layer, using carbon and Pt counter electrodes and FTO and ITO/glass, under AM 1.5 solar irradiation with a density of 100 mW/cm^2 (TiO_2 annealed at 450°C).

photovoltage (V_{oc}), and the fill factor for the FTO/glass substrate with Pt counter electrodes are greater than those of the other samples.

TABLE 3: Photovoltaic performance of DSSCs with sputtered compact TiO_2 layer, with carbon and Pt counter electrodes, using FTO and ITO/glass.

	V_{oc} (V)	J_{sc} (mA/cm^2)	Fill factor	Efficiency η (%)
FTO/sputter/spin coating/Pt	0.762	13.95	0.720	7.65
ITO/sputter/spin coating/Pt	0.622	12.38	0.647	4.98
ITO/sputter/spin coating/carbon	0.522	4.33	0.668	1.51

Conflict of Interests

The authors declare that there is no conflict of interests regarding the publication of this paper.

References

[1] M. Hamadanian, A. Gravand, and V. Jabbari, "High performance dye-sensitized solar cells (DSSCs) achieved via electrophoretic technique by optimizing of photoelectrode properties," *Materials Science in Semiconductor Processing*, vol. 16, pp. 1352–1359, 2013.

[2] H. Choi, E. Stathatos, and D. D. Dionysiou, "Photocatalytic TiO_2 films and membranes for the development of efficient wastewater treatment and reuse systems," *Desalination*, vol. 202, no. 1–3, pp. 199–206, 2007.

[3] D. Y. Chen, C. C. Tsao, and C. Y. Hsu, "Photocatalytic TiO_2 thin films deposited on flexible substrates by radio frequency (RF) reactive magnetron sputtering," *Current Applied Physics*, vol. 12, no. 1, pp. 179–183, 2012.

[4] H. Irie, Y. Watanabe, and K. Hashimoto, "Nitrogen-concentration dependence on photocatalytic activity of TiO_2-xNx powders," *Journal of Physical Chemistry B*, vol. 107, no. 23, pp. 5483–5486, 2003.

[5] Y. Nakano, T. Morikawa, T. Ohwaki, and Y. Taga, "Origin of visible-light sensitivity in N-doped TiO_2 films," *Chemical Physics*, vol. 339, no. 1–3, pp. 20–26, 2007.

[6] C.-G. Kuo and B.-J. Sheen, "Seaweed chlorophyll on the light-electron efficiency of DSSC," *Journal of the Chinese Chemical Society*, vol. 58, no. 2, pp. 186–190, 2011.

[7] Y.-L. Kuo, T.-L. Su, F.-C. Kung, and T.-J. Wu, "A study of parameter setting and characterization of visible-light driven nitrogen-modified commercial TiO_2 photocatalysts," *Journal of Hazardous Materials*, vol. 190, no. 1–3, pp. 938–944, 2011.

[8] B. O'Regan and M. Grätzel, "A low-cost, high-efficiency solar cell based on dye-sensitized colloidal TiO_2 films," *Nature*, vol. 353, no. 6346, pp. 737–740, 1991.

[9] K. R. Bae, C. H. Ko, Y. Park et al., "Structure control of nanocrystalline TiO_2 for the dye-sensitized solar cell application," *Current Applied Physics*, vol. 10, no. 3, pp. S406–S409, 2010.

[10] P.-C. Huang, C.-H. Huang, M.-Y. Lin, C.-Y. Chou, C.-Y. Hsu, and C.-G. Kuo, "The effect of sputtering parameters on the film properties of molybdenum back contact for CIGS solar cells," *International Journal of Photoenergy*, vol. 2013, Article ID 390824, 8 pages, 2013.

[11] J. H. Qi, Y. Li, T. T. Duong, H. J. Choi, and S. G. Yoon, "Dye-sensitized solar cell based on AZO/Ag/AZO multilayer transparent conductive oxide film," *Journal of Alloys and Compounds*, vol. 556, pp. 121–126, 2013.

[12] Y.-S. Jin, K.-H. Kim, W.-J. Kim, K.-U. Jang, and H.-W. Choi, "The effect of RF-sputtered TiO_2 passivating layer on the performance of dye sensitized solar cells," *Ceramics International*, vol. 38, no. 1, pp. S505–S509, 2012.

[13] C. G. Kuo, C. Y. Hsu, S. S. Wang, and D. C. Wen, "Photocatalytic characteristics of TiO_2 films deposited by magnetron sputtering on polycarbonate at room temperature," *Applied Surface Science*, vol. 258, pp. 6952–6957, 2012.

[14] H.-J. Kim, J.-D. Jeon, D. Y. Kim, J.-J. Lee, and S.-Y. Kwak, "Improved performance of dye-sensitized solar cells with compact TiO_2 blocking layer prepared using low-temperature reactive ICP-assisted DC magnetron sputtering," *Journal of Industrial and Engineering Chemistry*, 2012.

[15] H. Chang, T. L. Chen, K. D. Huang, S. H. Chien, and K. C. Hung, "Fabrication of highly efficient flexible dye-sensitized solar cells," *Journal of Alloys and Compounds*, vol. 504, no. 1, pp. S435–S438, 2010.

[16] H. Seo, M.-K. Son, J.-K. Kim, I. Shin, K. Prabakar, and H.-J. Kim, "Method for fabricating the compact layer in dye-sensitized solar cells by titanium sputter deposition and acid-treatments," *Solar Energy Materials and Solar Cells*, vol. 95, no. 1, pp. 340–343, 2011.

[17] C. G. Kuo, C. F. Yang, L. R. Hwang, and J. S. Huang, "Effects of titanium oxide nanotube arrays with different lengths on the characteristics of dye-sensitized solar cells," *International Journal of Photoenergy*, vol. 2013, Article ID 650973, 6 pages, 2013.

[18] Y. M. Sung, "Deposition of TiO_2 blocking layers of photovoltaic cell using RF magnetron sputtering technology," *Energy Procedia*, vol. 34, pp. 582–588, 2013.

[19] M. H. Abdullah and M. Rusop, "RF sputtered tri-functional antireflective TiO_2 (arc-TiO_2) compact layer for performance enhancement in dye-sensitised solar cell," *Ceramics International*, vol. 38S, pp. S505–S509, 2012.

[20] L. Zhang, Y. Zhu, Y. He, W. Li, and H. Sun, "Preparation and performances of mesoporous TiO_2 film photocatalyst supported on stainless steel," *Applied Catalysis B: Environmental*, vol. 40, no. 4, pp. 287–292, 2003.

[21] Y. Chen, E. Stathatos, and D. D. Dionysiou, "Sol-gel modified TiO_2 powder films for high performance dye-sensitized solar cells," *Journal of Photochemistry and Photobiology A: Chemistry*, vol. 203, no. 2-3, pp. 192–198, 2009.

[22] H. Tomaszewski, H. Poelman, D. Depla et al., "TiO_2 films prepared by DC magnetron sputtering from ceramic targets," *Vacuum*, vol. 68, no. 1, pp. 31–38, 2002.

[23] C. G. Kuo, C. F. Yang, M. J. Kao et al., "An analysis and research on the transmission ratio of dye sensitized solar cell photoelectrodes by using different etching process," *International Journal of Photoenergy*, vol. 2013, Article ID 151973, 8 pages, 2013.

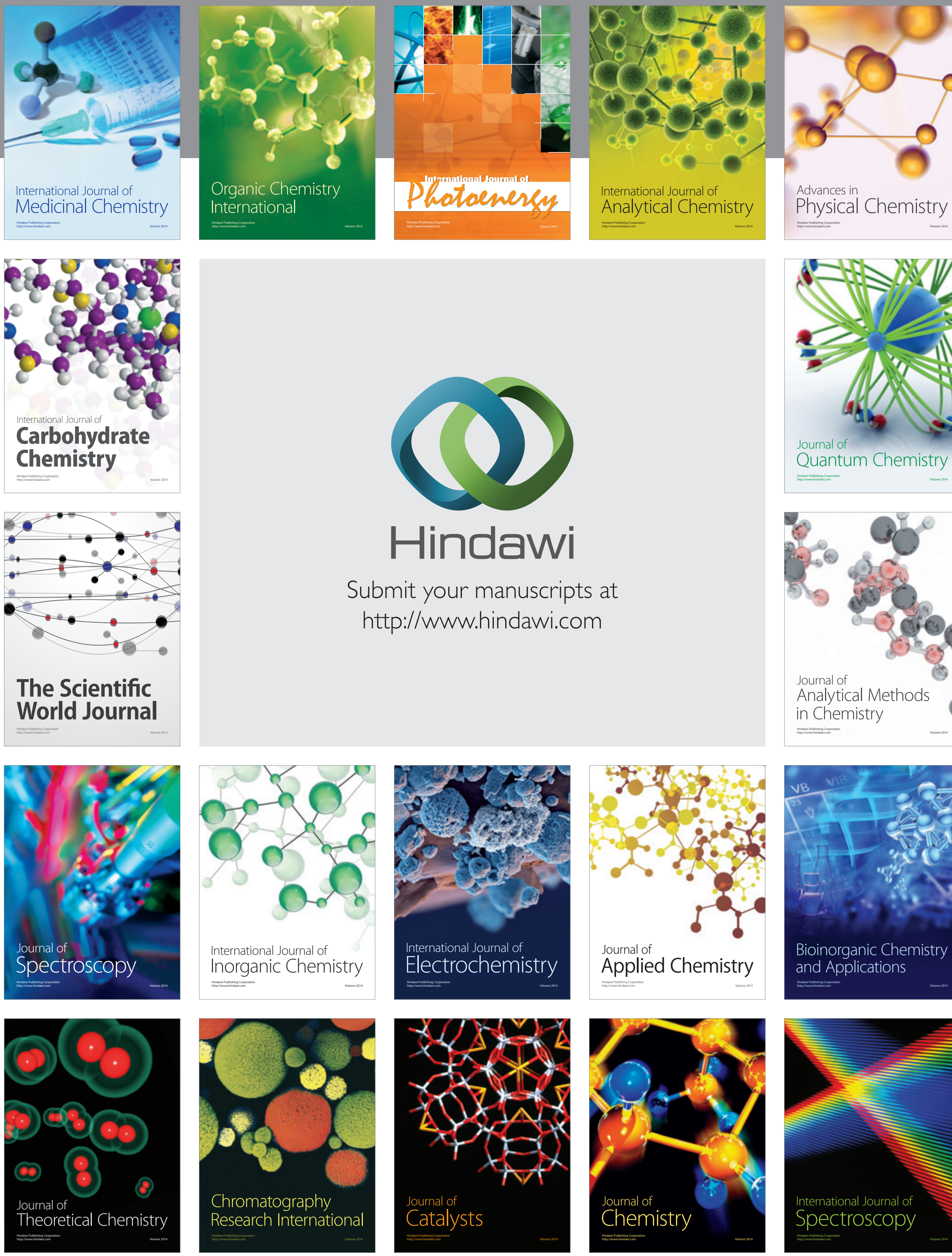
International Journal of Medicinal Chemistry
Organic Chemistry International
International Journal of Photoenergy
International Journal of Analytical Chemistry
Advances in Physical Chemistry
International Journal of Carbohydrate Chemistry
Hindawi
Submit your manuscripts at
http://www.hindawi.com
Journal of Quantum Chemistry
The Scientific World Journal
Journal of Analytical Methods in Chemistry
Journal of Spectroscopy
International Journal of Inorganic Chemistry
International Journal of Electrochemistry
Journal of Applied Chemistry
Bioinorganic Chemistry and Applications
Journal of Theoretical Chemistry
Chromatography Research International
Journal of Catalysts
Journal of Chemistry
International Journal of Spectroscopy